

Effects of Stress-Strain Characteristics on the Strength Of CHS X Joints

Seon-Hu Kim¹⁾, *Cheol-Ho Lee²⁾, Dong-Hyun Chung³⁾, Dae-Kyung Kim⁴⁾
and Jin-Won Kim⁵⁾

^{1), 2), 4)} *Department of Architecture and Architectural Engineering, Seoul National University, Seoul, Korea*

³⁾ *Dongyang Structural Engineers Group, Seoul, Korea*

⁵⁾ *Steel Solution Marketing Department, POSCO, Inchoen, Korea*

²⁾ *ceholee@snu.ac.kr*

ABSTRACT

Most of current steel design standards forbid or limit the use of high strength steels to tubular structures because of concerns about their unique stress-strain characteristics such as the absence of yield plateau and high yield ratio. The mechanical background of current limitations appears unclear and unduly conservative, and their validity needs to be re-evaluated. In this study, the effects of stress-strain characteristics were systematically investigated based on experimental and test-validated numerical analysis of CHS (circular hollow section) X joints fabricated from different steel grades of SM490, SM570, and HSA800. The strength of high strength steel joints was dominantly governed by the widely-accepted 3% indentation criteria long before reaching the peak strength. The joint strength often exceeded the EC3 nominal strength with sufficient margin, although the margin tended to decrease as the yield strength of steel became higher or as the brace to chord diameter ratio became smaller. Overall, the experimental and supplemental numerical results of this study indicated that high-strength steel CHS X joints show satisfactory performance, just slightly inferior to ordinary steels, from the perspective of serviceability, ultimate strength and ductility even when the yield strength of steel is as high as 800MPa.

1. INTRODUCTION

The use of circular hollow sections (CHSs) is being increased more and more in a wide range of structural applications because of their many technological advantages over open steel shapes and aesthetic appeal as well. The use of high-strength steel

^{1), 4)} Graduate Student

²⁾ Professor

³⁾ Assistant Manager

⁵⁾ Sr. Researcher

tubular members can bring about further advantages from design to erection. However, most of current internationally representative design standards such as 2008 CIDECT guide (Wardenier et al., 2008), 2010 AISC Specification (AISC, 2010), and EC3 (CEN, 2005) forbid or impose restrictions on the use of high strength steels for structures with hollow sections depending upon steel yield strength and/or yield ratio. The mechanical background of these limitations appears unclear and often unduly conservative, and their validity needs to be further investigated. As is well-known, current design standards for tubular joints were proposed based on the screened test database and extensive test-backed numerical results. Although fairly extensive experimental and associated analytical studies were conducted for CHS X joints in the past (for example, Sammet 1962, JSSC 1972, Gibstein 1973, Boone et. al 1982, Weinstein et al. 1986, Van der Vegte 1995, Kanatani 1996, Noordhoek et al. 1996 and others), the database on high strength steel joints is still quite limited. In this study, the effects of stress-strain characteristics were systematically investigated based on experimental testing and test-validated numerical analysis of CHS X joints fabricated from different steel grades of SM490, SM570, and HSA800 in order to augment the database and examine if current design standards could be extrapolated to high strength steels.

2. MATERIAL LIMITATIONS AND JOINT STRENGTH EQUATION

The limitations on steel materials and the joint strength equations for CHS X joints are first briefly summarized in this section. According to the 2010 AISC Specification, the applicable range of hollow section connection configuration is limited to steels whose yield strength (F_y) and yield ratio (F_u) are within 360 MPa and 0.8, respectively; the application of high strength steels to tubular structures is virtually forbidden. The joint resistances given in CIDECT guide are basically for steels with a nominal yield strength up to 355 MPa. For nominal yield strengths greater than this value, the joint resistances given should be multiplied by 0.9. However, the nominal specified yield strength should not exceed 460 MPa based on the finished tube product and should not be taken larger than $0.80F_u$, where F_u is the nominal ultimate tensile strength. The reduction factor 0.90 was introduced on one hand due to concerns about relatively larger deformations in CHS joints with F_y approaching 460 MPa and on the other hand probable lower deformation/rotation capacity of other joints with yield strengths exceeding 355 MPa (Wardenier et al., 2008). The CIDECT guide is more flexible and generous in that it provides some room for the application of high strength steels to tubular structures. EC3 (CEN 2005) gives additional rules for the use of very high strength steel or S700 whose nominal yield strength is 700 MPa. In this case, a reduction factor of 0.80 to the joint capacity equations has to be used instead of the factor 0.90.

Figure 1 shows typical geometrical configuration and the symbols of CHS X joints. Equation (1) below gives the generic form of the CHS X joint strength corresponding to the limit state of chord plastification. It is implied from equation (1) that the connection geometry and the chord stress are assumed to affect the joint strength in an uncoupled manner or in the form of $Q_u \times Q_f$. Table 1 summarizes the joint strength equation and range of applicability per EC3. Other standards also provide the joint strength provisions similar to EC3.

$$P_u = \frac{f_{y0} t_0^2}{\sin \theta} Q_u Q_f \quad (1)$$

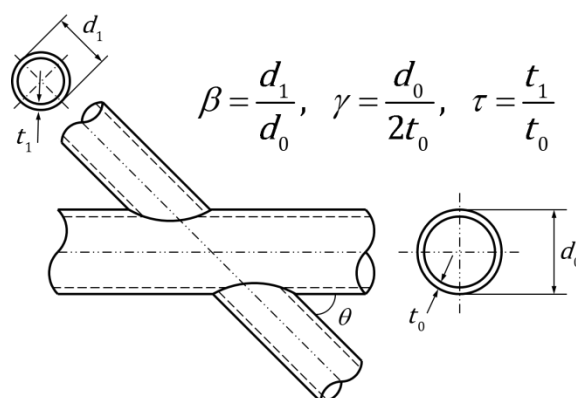


Figure 1: Geometrical configuration and definition of symbols of CHS X joints (see table 1 for the definition of Q_u and Q_f)

Table 1: Joint strength equation for CHS X joints: chord plastification limit state per EC3

Q_u (geometry factor)	Q_f (chord stress factor)		Range of applicability: material		Range of applicability: geometry		
	Chord in tension	Chord in compression	F_y	Yield ratio	β	2γ	θ
$\frac{5.2}{1 - 0.81\beta}$	1.0	$1 - 0.3n_p (1 + n_p) \leq 1.0^a$	355MPa ^b	0.9	0.2-1.0	≤ 50 (for $\theta < 90^\circ$) ≤ 40 (for $\theta = 90^\circ$)	$30^\circ - 90^\circ$

^a $n_p = \frac{\sigma_{p,Ed}}{f_{y0}}$ ($\sigma_{p,Ed}$: maximum compressive stress in the chord at a joint, f_{y0} : yield strength of a chord member.)

^b Steels whose yield strength is between 355MPa and 460MPa can be used with the reduction factor of 0.9, and steels from S460 up to S700 can be used with the reduction factor of 0.8.

3. EXPERIMENTAL PROGRAM

In this study, a total of 9 CHS X joints fabricated from cold-formed tubes were tested under axial compression. The key test variables included different grades of steels and geometrical configuration of the joint. Table 2 summarizes of the material and geometric properties of the test specimens. In order to investigate the effect of different steel material dimensions on the X joint behavior, one ordinary steel SM490 ($F_y = 325\text{MPa}$ and $F_u = 490\text{MPa}$), two high strength steels SM570 ($F_y = 420\text{MPa}$ and $F_u = 570\text{MPa}$) and HSA800 ($F_y = 650\text{MPa}$ and $F_u = 800\text{MPa}$) were included. Especially, HSA800 is a high-strength steel recently developed in Korea through the thermo-mechanical control process (TMCP) for building applications. HSA800 has a tighter control on material properties as it specifies an upper limit on the yield ratio (0.85) as well as tensile strengths and has lower carbon equivalent content for improved weldability compared to conventional quenching/tempering high strength steels. Please refer to Lee et al. (2013) and Kim et al. (2014) for more details of this steel. Note that SM570 and HSA800 are not permitted for tubular structures according to the 2010 AISC Specification. However, these steels may be used with applying a suitable joint strength reduction factor by following the procedure of CIDECT guide or EC3 mentioned in the previous section.

Table 2: Summary of material and geometric properties of test specimens

Test Specimen ^a	Chord length l_0 (mm)	Brace angle θ (in degrees)	Nominal yield strength F_y (MPa)	Nominal tensile strength F_u (MPa)	Geometric parameters					
					d_0 (mm)	t_0 (mm)	d_1 (mm)	t_1 (mm)	β	2γ
X90-325-0.75-16	3000	90	325	490	400	25	300	15	0.75	16
X90-325-0.62-26	2500				650	25	400	25	0.62	26
X90-420-0.62-26	2500	90	420	570	650	25	400	25	0.62	26
X90-650-0.75-16	3000				400	25	300	15	0.75	16
X90-650-0.62-26	2500	90	650	800	650	25	400	25	0.62	26
X60-325-0.62-26	3000				650	25	400	25	0.62	26
X60-420-0.62-26	3000	60	420	570	650	25	400	25	0.62	26
X60-650-0.62-26	3000				650	25	400	25	0.62	26
X45-650-0.62-26	3000	45	650	800	650	25	400	25	0.62	26

^a In the specimen identification, the first character X represents X joint, and is followed by the brace to chord angle θ , the nominal yield strength of steel F_y , the brace to chord diameter ratio β , and the chord diameter to thickness ratio 2γ .

As can be seen in Table 2, the key geometric parameters $\beta (= d_1 / d_0)$, $2\gamma (= d_0 / t_0)$, $\tau (= t_1 / t_0)$, and θ are all within the valid ranges of EC3 provisions (see

Table 1). The brace to chord diameter ratio β was chosen as 0.62 and 0.75 to induce chord plastification. The stress-strain diagrams obtained from the coupons of each steel plate (or before press bending) are plotted in Figure 2. As expected, Figure 2 shows that SM490, as an ordinary-strength steel, has a stress-strain characteristics desirable for ductile behavior at member and structural levels; they have a sharp yield point, a distinct yield plateau, significant strain-hardening, and a low yield ratio. However, the two high strength steels, SM570 and HSA800, lack these properties. Recently the effects of these different post-elastic properties on the strength and the rotation capacity of I-shaped beams were experimentally and analytically investigated by Lee et al. (2013). This study may be viewed as an attempt to investigate such effects on CHS X joints.

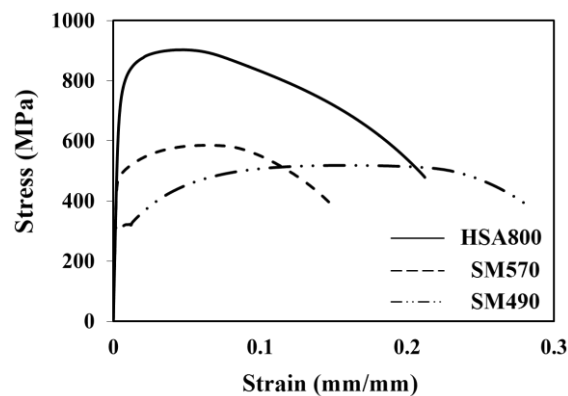


Figure 2: Measured stress-strain diagrams

Figures 3a and 3b show an overall view of typical test setup. A universal testing machine of 10,000 kN capacity was used to apply pseudo-static axial compression to the X joint specimens. Both ends of the chord were set free except the lateral restraint provided to prevent out-of-plane displacement if any. No load was applied to the chord; or all the tests were conducted under the condition of the chord stress factor (Q_f) of 1.0. A total of six LVDTs were attached around the joint to measure the out-of-face deformations at the saddle and crown points (see Figure 3c). Additional LVDTs were also provided to measure global displacements of brace and chord members. A lot of strain gages were installed around the joint to monitor more detailed behavior.

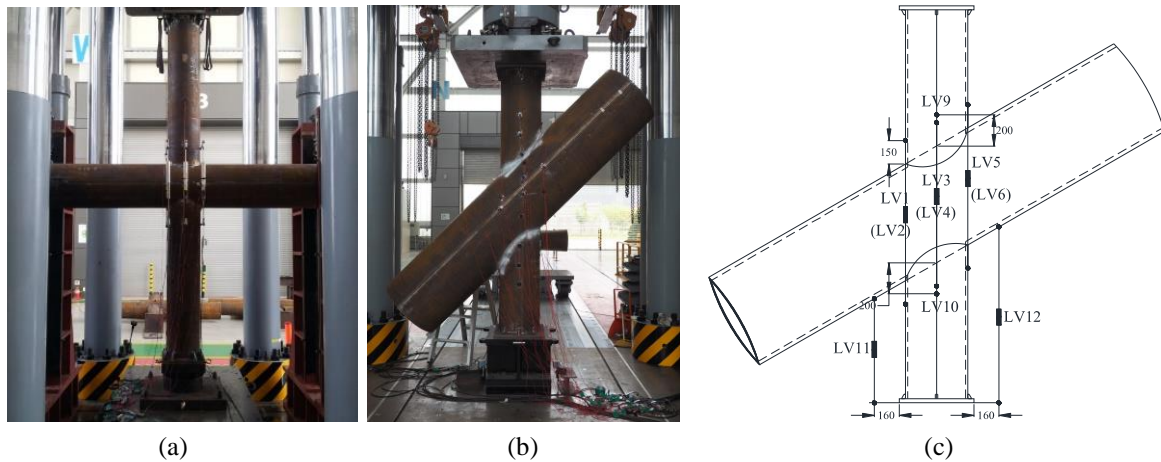


Figure 3: Typical test setup and LVDT arrangement: (a) X90-650-0.75-16; (b) X-45-0.62-26; (c) LVDT arrangement

4. SUPPLEMENTAL NUMERICAL ANALYSIS PROGRAM

In order to supplement the limited test database of this study, test-validated FE (finite element) numerical analyses were also conducted. With the same steel grades used in the test (SM490, SM570 and HSA800), and by varying β ($\beta = 0.20, 0.40, 0.62,$ and 0.80), a total of 12 numerical models with $\theta = 90^\circ$ were created and analyzed. Table 3 summarizes the material and geometric information of the numerical models investigated. Especially, the three models with $\beta = 0.62$, X90-325/420/650-0.62-26 (N) in Table 3 were used in validating the accuracy of FE numerical modeling of this study. Note that the chord geometries and the brace thicknesses are all kept identical.

Table 3. Material properties and geometric dimensions for FE numerical analysis models

Numerical model ^a	Chord length l_0 (mm)	Brace angle θ (in degrees)	Nominal yield strength F_y (MPa)	Nominal tensile strength F_u (MPa)	Geometric parameters					
					d_0 (mm)	t_0 (mm)	d_1 (mm)	t_1 (mm)	β	2γ
X90-325-0.20-26 (N)			325	490						
X90-420-0.20-26 (N)			420	570			130	25	0.2	
X90-650-0.20-26 (N)			650	800						
X90-325-0.40-26 (N)			325	490						
X90-420-0.40-26 (N)			420	570			260	25	0.4	
X90-650-0.40-26 (N)	2500	90	650	800	650	25				26
X90-325-0.62-26 (N)			325	490						
X90-420-0.62-26 (N)			420	570			400	25	0.62	
X90-650-0.62-26 (N)			650	800						
X90-325-0.80-26 (N)			325	490						
X90-420-0.80-26 (N)			420	570			520	25	0.8	
X90-650-0.80-26 (N)			650	800						

^a The same naming rule used for the specimen identification in Table 2 was again applied for the numerical model.; the last character N in the parenthesis stands for numerical analysis.

Numerical analysis was done using the commercial FE software ABAQUS (Simulia, 2014). First, validation of FE numerical model was carried out by using experimental results obtained from the three test specimens X90-325/420/650-0.62-26 (see Table 2). For the material option, the von Mises yield criterion with isotropic hardening was assumed and the 20-node solid elements with reduced integration (C3D20R in ABAQUS) were used to ensure a sufficient degree of accuracy, rather than more *cheap* 8-node solid element or shell element. RIKS algorithm was employed as static analysis option in order to trace unstable behavior if any. The weldment as fabricated was reflected in the FE modeling. But geometric imperfection was not considered because the behavior of CHS X-joints were shown to be geometric-imperfection insensitive. Mesh sensitivity study was also conducted to assure convergence. The load-indentation deformation responses predicted by the FE modeling scheme described above showed excellent correlation with experimental results of the three CHS X joints with $\beta = 0.62$ (see Figure 6c).

5. DISCUSSIONS OF EXPERIMENTAL AND NUMERICAL RESULTS

2.1 Joint strength criteria and joint ductility

Before presenting the results, the joint strength criteria is briefly reviewed first.

The joint strength in many design standards (e.g., CIDECT guide) is based on the ultimate limit state and is defined by the lower of the ultimate strength of the joint and the load corresponding to an ultimate deformation limit. An out-of-plane deformation of the connecting face, equal to 3% of the CHS face diameter ($3\%d_0$) is generally used as the ultimate deformation limit by following the recommendation by Lu et al. (1994). This serves to control joint deformations at both the factored and service load level, which is necessary due to concerns about some highly flexible CHS joints. This ultimate deformation limit implicitly aims at restricting joint deformation at service load less than $1\%d_0$. In proposing this ultimate deformation limit by Lu et al (1994), the factored to service load ratio was assumed to be 1.50. In current steel design practice, this ratio is usually taken as 1.67 or 1.70 (e.g., AISC 2010). It seems that the $3\%d_0$ ultimate deformation limit is widely adopted among researchers for all types of welded tubular joints.

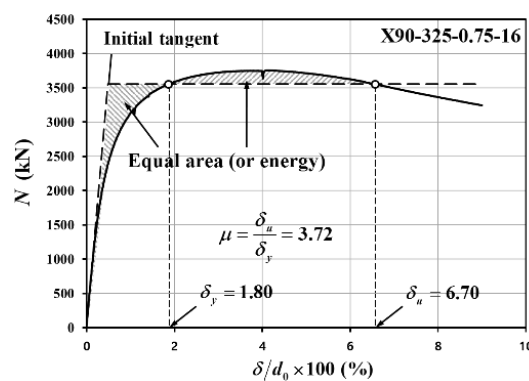


Figure 4: Definition of connection ductility (μ) proposed based on equal energy criteria

The joint ductility (μ) or energy absorption capacity is crucially important under extreme loading events for a structure to survive through redistribution of forces. The joint ductility may be defined in a somewhat varied manner depending upon joint type and application purposes. Within the authors' knowledge, a universally accepted definition for the ductility of tubular joints appears not available. In order to appraise the joint ductility on a common basis, the definition of ductility for CHS X joints is temporarily proposed in this study. Since the load-deformation relation of CHS X joints is geometrically nonlinear from the beginning, the definition is proposed based on the initial tangent and the equal energy criteria as illustrated in Figure 4. Defining the ductility in this manner is a bit arbitrary, but it is believed that the joint ductility can be compared in a consistent manner from this definition.

Table 4: Summary of experimental and supplemental numerical analysis results ($\theta = 90^\circ$)

Numerical model or test specimen ^a	β	Tensile mechanical properties after press bending			Experimental or numerical joint strength (kN)		Standard-nominal joint strength based on measured yield strength (kN)			Joint strength normal- ized by EC3 formula	μ^c
		Measured yield strength (MPa)	Measured tensile strength (MPa)	YR	Experimental or numerical joint strength (kN)		AISC	CIDECT	EC3		
					3% d_0	Peak					
X90-325-0.20-26 (N)		324	518	63%	1421	1422 (3.3% ^b)	1240	1079	1257	13%	3.49
X90-420-0.20-26 (N)	0.20	478	586	82%	1942	1967 (3.7%)	NA	NA	1483	31%	2.23
X90-650-0.20-26 (N)		798	914	82%	2666	2922 (4.8%)	NA	NA	2476	7%	1.98
X90-325-0.40-26 (N)		324	518	63%	1975	1982 (3.6%)	1537	1504	1558	27%	3.34
X90-420-0.40-26 (N)	0.40	478	586	82%	2773	2819 (4.0%)	NA	NA	1838	51%	2.80
X90-650-0.40-26 (N)		798	914	82%	3949	4295 (5.1%)	NA	NA	3069	28%	2.52
X90-325-0.62-26 (N)		324	518	63%	2673	2678 (3.5%)	2089	2216	2117	26%	3.78
X90-325-0.62-26 (E)		324	518	63%	2640	2660 (4.0%)	2089	2216	2117	25%	3.88
X90-420-0.62-26 (N)	0.62	478	586	82%	3800	3827 (3.7%)	NA	NA	2497	52%	3.21
X90-420-0.62-26 (E)		478	586	82%	3759	3839 (4.2%)	NA	NA	2497	51%	3.21
X90-650-0.62-26 (N)		798	914	82%	5611	5869 (4.8%)	NA	NA	4166	35%	2.78
X90-650-0.62-26 (E)		798	914	82%	5612	5900 (4.9%)	NA	NA	4166	35%	2.70
X90-325-0.80-26 (N)		324	518	63%	3803	3805 (3.2%)	2951	3165	2991	27%	4.29
X90-420-0.80-26 (N)	0.80	478	586	82%	5287	5288 (2.9%)	NA	NA	3531	50%	3.63
X90-650-0.80-26 (N)		798	914	82%	7960	7998 (3.7%)	NA	NA	5894	35%	3.47

^a E = experimental, N = numerical.

^b The out-of-plane deformation of the crown in terms of % d_0 at peak load.

^c Joint ductility. See Figure 4 for the definition.

5.2 Discussions

Experimental and numerical results of this study were evaluated according to the joint strength criteria proposed by Lu et al (1994) discussed above. The joint strengths and joint ductility obtained from both test and numerical results are summarized in Table 4. In preparing Table 4, following aspects were considered. The AISC and CIDECT nominal strengths for SM570 and HSA800 specimens were not provided since their yield strengths all violated the upper limits of the yield strength; 355MPa (AISC) and 460MPa (CIDECT). The nominal joint strengths for SM570 and HSA800 specimens were calculated with including the reduction factor of 0.80 according to the additional rules for steels with grades higher than S460 and up to S700 in EC3, since their measured yield strengths ranged from 478 to 798MPa (see Table 4). All the nominal joint strengths were computed by using the measured yield strength reported in Table 4. It is noted that all the three standards specify similar joint strengths. The joint strengths in this study was mostly governed by the 3% d_0 criteria except X90-420-0.80-26(N) with $\beta = 0.80$.

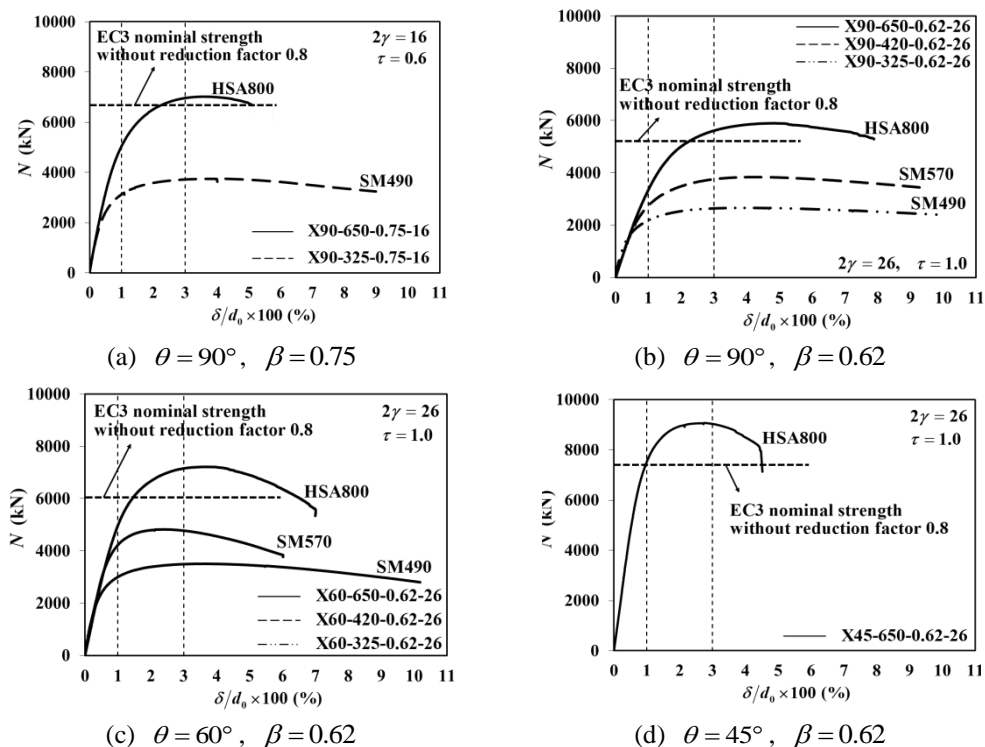


Figure 5: Load versus out-of-deformation relationships obtained from experiments

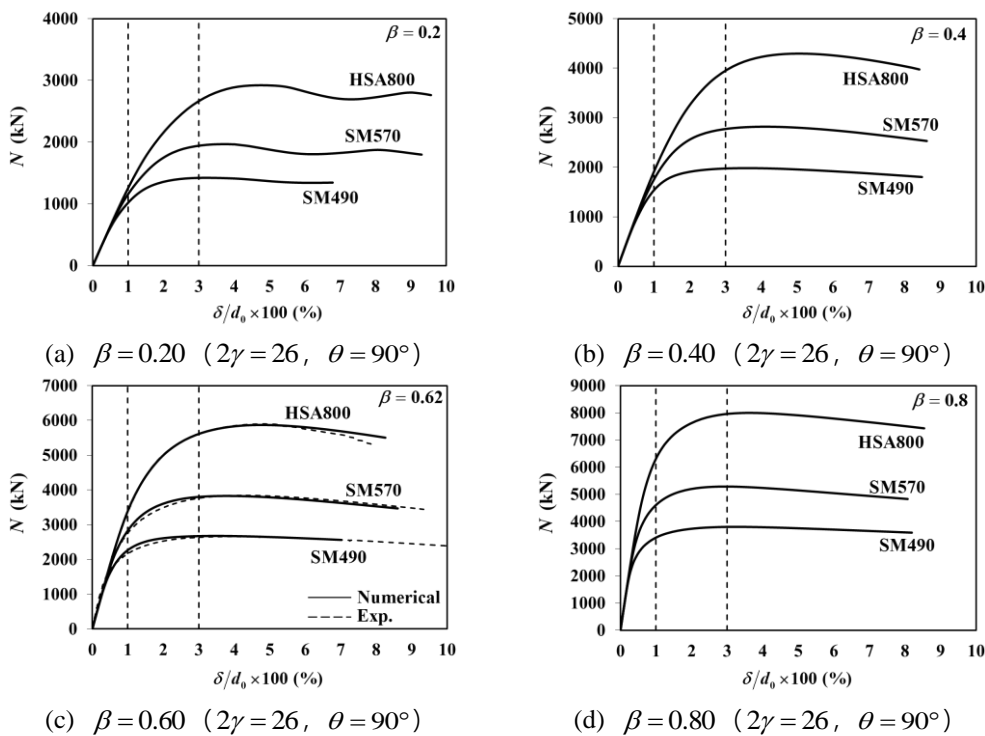


Figure 6: Load versus out-of-deformation relationships obtained from numerical analysis

Figure 5 and Figure 6 respectively show the axial compression versus out-of-deformation curves obtained from test and numerical analysis. As can be observed in Figure 5, EC3 nominal strength equation still underestimates the experimental strengths of HSA800 specimens even when the reduction factor 0.8 is not applied. Table 4 indicates that all the joint strengths exceed the EC3 nominal strength, often with sufficient margin, although the margin tended to decrease as the yield strength of steel became higher or as the brace to chord diameter ratio became smaller. This may be explained in terms of more localized out of bending deformation of the chord face and reduced force transfer to the side wall of the chord when brace to diameter ratio becomes smaller (say, $\beta = 0.20$ is involved). It is interesting to note that the strength margin for test specimens and numerical models with SM570 is particularly high. It seems that this conspicuous conservatism is just artificial because the measured yield strength of SM570 (478MPa) is just slightly above the threshold strength (460MPa) for which the highest reduction factor 0.8 should be applied.

Table 4 also shows the joint ductility of all models. Overall, it may be said that each joint exhibits comparable order of ductility ranging from 2 and 4. However, surely the joints with high strength steels (SM570 and HSA800) show smaller ductility compared to ordinary steel (SM490). For SM490, the joint ductility ranges from 3.5 to 4.3. For SM570 and HSA800, it is in the order of 2.2 to 3.6 and 2.0 to 3.5, respectively.

Table 5: Out-of-plane deformation ($\%d_0$) corresponding to service load level $N_s = N_u^a / 1.5$ or

$$N_s = N_u^a / 1.7$$

Steel grade	Numerical model or test specimen	$\% d_0$	
		$N_s = N_u / 1.5$	$N_u / 1.7$
SM490	X90-325-0.20-26 (N)	0.89%	0.74%
	X90-325-0.40-26 (N)	0.78%	0.66%
	X90-325-0.62-26 (N)	0.59%	0.48%
	X90-325-0.62-26 (E)	0.53%	0.41%
	X90-325-0.80-26 (N)	0.38%	0.30%
SM570	X90-420-0.20-26 (N)	1.17%	0.98%
	X90-420-0.40-26 (N)	1.08%	0.91%
	X90-420-0.62-26 (N)	0.82%	0.68%
	X90-420-0.62-26 (E)	0.84%	0.67%
	X90-420-0.80-26 (N)	0.50%	0.40%
HSA800	X90-650-0.20-26 (N)	1.51%	1.29%
	X90-650-0.40-26 (N)	1.48%	1.26%
	X90-650-0.62-26 (N)	1.15%	0.96%
	X90-650-0.62-26 (E)	1.16%	0.98%
	X90-650-0.80-26 (N)	0.71%	0.59%

^a N_u is experimental or numerical joint strength reported in Table 4

As mentioned previously, the $3\%d_0$ ultimate deformation limit proposed by Lu et al. (1994) also aims at restricting the joint deformation at service load less than $1\%d_0$. In proposing this ultimate deformation limit, the factored to service load ratio was assumed to be 1.50. In current steel design practice, this ratio is usually taken as 1.67 or 1.70 (e.g., AISC 2010). Table 5 summarizes the out-of-plane deformation ($\%d_0$) corresponding to service load level $N_s = N_u/1.5$ or $N_u/1.7$. Table 5 shows that as the strength of steel becomes higher, the deformation level tends to increase. For the factored to service load ratio of 1.5, some of SM570 joints and most of HSA800 joints violated the $1\%d_0$ deformation criteria at service load. However, for the ratio of 1.7, most of the joints satisfy the deformation criteria for serviceability except HSA800 joints with $\beta = 0.20$ and $\beta = 0.40$. Although HSA800 joints with small β do not meet the serviceability criteria, considering that the value of β is usually larger than 0.5~0.6 in practice, this slight violation appears a minor issue subjected to engineering judgement.

Considering all these, it may be said that both test specimens and supplementary numerical models with high strength steels in this study exhibit acceptable in terms of serviceability, strength, and ductility.

6. SUMMARY AND CONCLUSIONS

In this study, the effects of different stress-strain characteristics on the structural performance of CHS X joints investigated experimentally and numerically by using typical ordinary and high strength steels. The primary objective was to explore the possibility of extrapolating current ordinary-steel based design standards to high strength steels. The results of this study can be summarized as follows.

i) The benchmark steel, SM490, showed a stress-strain characteristics typical of an ordinary-strength steel with a sharp yield point, a distinct yield plateau, and a yield ratio as low as 0.62. Whereas the two high strength steels, SM570 and HSA800, lacked such properties and had the yield strength of 478 and 798MPa respectively, thus falling into the category for which the joint strength reduction factor 0.80 should be applied according to the EC3 rule.

ii) All of the high-strength steel X joints exceeded the EC3 nominal strength, often with sufficient margin, although the yield strength of steel was as high as 800MPa. Generally, the margin was higher for high strength steels as a result of applying the joint strength reduction factor 0.80 according to the EC3 rule, except the case where the brace to chord diameter ratio (β) approached the lower limit 0.2.

iii) Particularly high conservatism observed in SM570 joint models is just artificial because the measured yield strength of SM570 (478MPa) is just slightly above the threshold strength (460MPa) from which the highest reduction factor 0.8 should be applied. More smooth variation of the joint strength reduction factor from 0.90 to 0.80, depending upon the yield strength of steel, would lead to more uniformity in conservatism.

iv) As the yield strength of steel becomes higher, the deformation at service load level tends to increase. For the factored to service load ratio of 1.5, HSA800 joints violates the $1\%d_0$ deformation criteria by about 50% when β is less than 0.4. However, for the ratio of 1.7, almost all of the high-strength steel joints satisfy the deformation criteria for serviceability except HSA800 joints with β less than 0.4. Considering that the value of β is usually higher than 0.5~0.6 in practice, this slight violation appears as a minor issue subjected to engineering judgements.

v) Based on the definition of joint ductility proposed in this paper for a consistent comparison, the ductility of CHS X joints with SM490, SM570 and HSA800 was respectively 3.76, 3.02, and 2.69 on average. Although the ductility tends to decrease as the yield strength of steel becomes higher, high strength steel CHS X joints seem to have still acceptable order of ductility.

Considering all these, it may be said that the high strength steel CHS X joints of this study showed an acceptable performance in terms of serviceability, strength, and ductility, although further test and supplemental numerical studies are needed to draw more general conclusions.

ACKNOWLEDGEMENT

This research was supported by a grant from High-Tech Urban Development Program (2009 A01) funded by Ministry of Land, Infrastructure and Transport of Korea. Additional support to this study by the POSCO Affiliated Research Professor Program is also gratefully acknowledged.

REFERENCES

[1] Wardenier, J., Kurobane, Y., Packer, J.A., Vegte, G.J. van der, & Zhao, X.-L.

- (2008). Design guide for circular hollow section (CHS) joints under predominantly static loading. Construction with hollow steel sections, 2nd ed., No. 1. *CIDECT*.
- [2] AISC (2010). Specification for Structural Steel Buildings. *American Institute of Steel Construction*.
- [3] CEN (2005). Eurocode 3: Design of steel structures, Part 1.8: Design of joints. *Brussels: European Committee for Standardization*.
- [4] Sammet, H. (1962). Die festigkeit kastenblechlasar rohrerbundungem in stahlbau zeitschrift zor alle Gebiete de Scwaws. *Schnied und Lotteohnik*, 13, 481-485.
- [5] JSSC (1972). Study of tubular joints used in marine structures. *The Society of Steel Construction of Japan*.
- [6] Gibstein, M. B. (1973). Static strength of tubular joints. *Det norske Veritas, Report*, 73-86.
- [7] Boone, T. J., Yura, J. A., & Hoadley, P. W. (1982). Chord stress effects on the ultimate strength of tubular joints. *PMFSEL Report No. 82-1*. University of Texas at Austin.
- [8] Weinstein, R. M., & Yura, J. A. (1986). The effect of chord stresses on the static strength of DT tubular connections. In *Offshore Technology Conference*. Offshore Technology Conference.
- [9] Van der Vegte, G. J. (1995). *The static strength of uniplanar and multiplanar tubular T-and X-joints*. TU Delft, Delft University of Technology.
- [10] Kanatani, H. (1966). Experimental study on welded tubular connections. *Faculty of Engineering Report*, 12, 13-41.
- [11] Noordhoek, C., Verheul, A., Foeken, R. J., Bolt, H. M., & Wicks, P. J. (1996). Static strength of high strength steel tubular joints. *ECSC agreement number 7210-MC, 602*.
- [12] Lee, C. H., Han, K. H., Uang, C. M., Kim, D. K., Park, C. H., & Kim, J. H. (2012). Flexural strength and rotation capacity of I-shaped beams fabricated from 800-MPa steel. *Journal of Structural Engineering*, 139(6), 1043-1058.
- [13] Kim, D. K., Lee, C. H., Han, K. H., Kim, J. H., Lee, S. E., & Sim, H. B. (2014). Strength and residual stress evaluation of stub columns fabricated from 800MPa high-strength steel. *Journal of Constructional Steel Research*, 102, 111-120.
- [14] Lu, L. H., De Winkel, G. D., Yu, Y., & Wardenier, J. (1994). Deformation limit for the ultimate strength of hollow section joints. In *Proc. Sixth International Symposium on Tubular Structures*, 341-347.
- [15] Simulia (2014). *Abaqus 6.14: Abaqus/CAE User's Guide*. Dassault Systemes, Providence, RI.